Determination of Phenylthiohydantoin–Amino Acids by Two-Step Laser Desorption/Multiphoton Ionization

Friedrich Engelke,[1] Jong Hoon Hahn, Wolfgang Henke, and Richard N. Zare*

Department of Chemistry, Stanford University, Stanford, California 94305

The 20 primary phenylthiohydantoin (PTH)–amino acids can be detected and quantitated by time-of-flight (TOF) mass spectrometry using a two-step laser methodology. First a CO_2 laser pulse desorbs the PTH–amino acid or a mixture thereof prepared as a thin film on the inside wall of a rotating glass cup. The latter is part of the first electrode of the TOF apparatus. The desorption process is demonstrated to be essentially complete in the laser spot area. After a suitable time delay, a second UV laser pulse (266 nm) causes 1 + 1 resonance-enhanced multiphoton ionization (REMPI) of the neutral cloud of desorbed molecules. The mass spectra obtained are dominated by the parent ion peak in almost all cases. Knowledge of the velocity distribution permits flux measurement. The ion signal is linear in PTH–amino acid concentration in the range of picomoles to nanomoles. This is the first demonstration of quantitative analysis of molecules by laser desorption/multiphoton ionization.

The development of laser-based analytical methods in recent years has been rapid (*1–4*). Particularly dramatic has been the explosive growth in laser-assisted mass spectrometry (*5*). The most severe limitation in the mass spectral analysis of thermally labile or highly polar compounds is that thermal evaporation of the sample is required. In most cases the energy needed for the evaporation step exceeds that for thermal degradation. Primarily for this reason many biologically important substances are intractable in analysis by classical mass spectrometric methods.

A number of exciting new developments including condensed-phase ejection-ionization methods like thermal desorption (*6*), field desorption (*7*), plasma desorption (*8*), laser desorption (LD) (*9–17*), sputtering of substances as secondary ions by bombardment with energetic primary ions (SIMS) (*18, 19*) or atoms (FAB) (*20*), thermospray (*21, 22*), and electrospray (*23*) have been reported in recent years. All these techniques have in common ions that are created directly out of the condensed phase by photon (*9–17, 24–26*), fast atom (*20*), or ion impact (*18, 19*); i.e., there is no distinction between desorption and ionization. As most of the desorbed material is in the neutral rather than in the ionic state, where the ion to neutral ratio is in the range of 10^{-3}–10^{-5}, postionization of neutral species in the gas phase by a second laser pulse is the next logical step (*12, 27–31*).

Here we present results demonstrating a two-step laser desorption/laser ionization process followed by time of flight (TOF) mass spectrometry. This has been applied to the determination of phenylthiohydantion (PTH)–amino acids, the final derivative in the sequencing of proteins by the Edman degradation method (*5, 32, 33*). High-performance liquid chromatography (HPLC) is by far the most widely used method for PTH–amino acid analysis (*34*). A sensitivity of 5 pmol was reported by UV absorption (*35*). Because HPLC intrinsically requires a long running time and identification is based only on retention times, work is in progress to interface HPLC separation with identification (*36*) of the PTH–amino acids. Recently, a sensitivity of 100 pmol has been obtained by SIMS (*37*).

The key to our methodology is the spatial and temporal separation of desorption and ionization. This allows us to select the energies and pulse durations for each of these two steps independently. By choosing suitable parameters for both lasers, we are able to make the detection of the PTH–amino acids quantitative with a linear response over several orders of magnitude in concentration. Moreover, the use of 1 + 1 resonance-enhanced multiphoton ionization (REMPI) in which one photon causes electronic excitation of the PTH–amino acid and a second photon causes ionization of the excited state is both highly selective and efficient. The high sensitivity of REMPI combined with the small amount of sample needed in the desorption step should allow the use of this method to analyze samples of biologically important molecules with a detection limit in the picomole range or less.

EXPERIMENTAL SECTION

Procedure. Two-Step LD/REMPI Technique. After the sample is introduced into the vacuum system, as a first step a CO_2 laser beam is directed to the thin film of the sample deposited on the inner surface of a rotating glass cup. Neutral molecules are generated in a fast desorption process. The cloud of desorbed molecules then expands into the high vacuum between two electrodes that form the acceleration region of a simple linear TOF mass spectrometer. In the second step these molecules are ionized by REMPI with an ultraviolet laser (Nd:YAG laser at 266 nm). The appropriate delay between the desorbing CO_2 laser and the ionizing Nd:YAG laser pulse is chosen so that the ionizing laser pulse intercepts as many molecules as possible.

Apparatus. Figure 1 clarifies the construction of our experimental apparatus, which consists of a home-built TOF mass spectrometer in a vacuum system. The extraction field of the TOF mass spectrometer was 130 V/cm, the (second) acceleration field was 400 V/cm, the draft tube was at −1.4 kV, and the mean flight path was 0.3 m. The vacuum system consists of a small standard turbo pump (50 L/s), which exhausts a six-port 4-in. stainless-steel cross. With the help of two additional liquid N_2 traps, the residual pressure did not exceed 10^{-6} torr during the experiment. A pulsed CO_2 laser (Pulse Systems LP 30; 10 Hz, multiline, $\lambda \simeq 10.6$ μm) with an internally mounted aperture (10 mm d.) is focused by a ZnSe lens (f = 250 mm) onto the inner surface of a rotatable glass cup under a 45° angle. The cup is placed in the center of the first electrode of our TOF mass spectrometer. The desorbed molecules in an expanding cloud directed toward the axis of the TOF mass spectrometer are irradiated at right angles by a frequency-quadrupled Nd:YAG laser (Quanta Ray) of 266 nm wavelength; in most of our experiments the Nd:YAG laser was slightly focused by a quartz lens to a diameter of 6 mm resulting in a power density of about 10^6 W/cm^2 in the ionization volume. The laser pulse width is 10 ns, which is most suitable for TOF analyses. The timing is as follows: A first pulse from the Nd:YAG laser clock with an appropriate delay and amplification triggers the CO_2 laser. A second pulse from a fast photodiode irradiated by the Nd:YAG laser pulse triggers an oscilloscope and our data acquisition system. The ions formed in the acceleration region of the linear TOF mass spectrometer

[1] Permanent address: Department of Physics, University of Bielefeld, D4800 Bielefeld, Federal Republic of Germany.

0003-2700/87/0359-0909$01.50/0

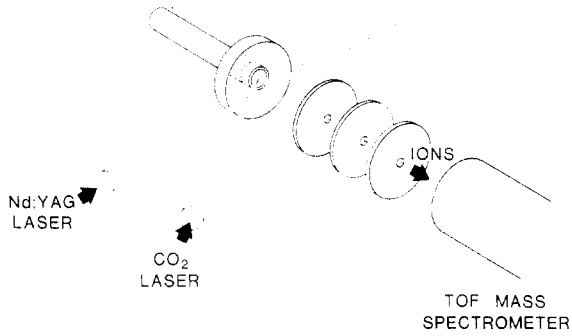

Figure 1. Schematic of the two-step laser desorption/multiphoton ionization setup. CO_2 laser desorption is performed at the inner surface of a rotating glass cup in the first electrode, i.e., the first acceleration region of a time-of-flight mass spectrometer. A 266-nm laser beam acts as an ionizing laser.

Table I. Typical Operating Parameters

CO_2 laser fluence (λ 10.6 μm, τ_p = 10 μs)	$\lesssim$200 mJ/cm^2
Nd:YAG laser fluence (freq quadrupled, λ 266 nm, τ_p = 10 ns)	$\lesssim$1 mJ/cm^2
acceleration voltage	1.6 kV
multiplier voltage	2 kV–3 kV–4 kV
gain	2×10^4–2×10^5–1×10^6
TOF mass spectrometer resolution	80 (10% valley)
pressure inside TOF mass spectrometer	$<10^{-6}$ torr
probe rotation	$2\pi/90$ s^{-1}
duty cycle	10 Hz

are then analyzed by an ion current measurement with a 21-stage CuBe electron multiplier (amplification factor of about 10^6) in connection with a fast preamplifier (ORTEC, Model 9301). The signals are stored and further processed by a waveform recorder (LeCroy, Model 9400) and plotted. A complete mass spectrum is obtained for each CO_2/Nd:YAG laser shot in a few microseconds. Most of the spectra obtained and represented here are the average over 100 laser pulses ($\sim$10 s). Table I presents the main operation parameters. The fixed-laser fluences are reported together with the TOF mass spectrometer characteristics.

Reagents and Sample Preparation. The chemicals used in our experiment were obtained from Sigma Chemical Co. and Pierce Chemical Co. and used without further purification. PTH-arginine and PTH-cysteic acid were obtained from commercially available salts with the treatment of NaOH and HCl, respectively, followed by extraction with ethyl acetate. The sample was generally dissolved in ethyl acetate. These dilutions provided the different PTH-amino acids (or mixtures containing different PTH-amino acids) at known concentrations. Application of a given volume (usually 100 μL) of the dilution to our rotating cup gave a convenient sample size of each PTH-amino acid for quantitative measurements. PTH-amino acid and solvent additions are made via a thin tube which delivers the solution at the bottom of the glass cup. As the solution emerges from the tube, it is spun by centrifugal force onto the wall and spread out as a thin film over the inner surface. Volume of liquid for a given time is metered so that the level is sufficient just to cover the inner surface. A vacuum is applied to remove the solvent leaving a dry PTH-amino acid film. The thickness of our samples varied from hundreds of monolayers—easily visible by eye—to submonolayer. One monolayer of the sample molecules on the glass substrate corresponds to about 10 pmol in the desorbing CO_2 laser area of 0.01 cm^2. After evaporation of the solvent, the glass cup is mounted onto a $^1/_2$ in. diameter Teflon rod and introduced into the TOF mass spectrometer through one of the vacuum locks. In order to prevent the main vacuum system from being directly exposed to the atmosphere when we introduce the sample into the system, a small rough-vacuum chamber, the volume of which is about 20 cm^3, has been equipped in front of the high-vacuum gate valve. It allows us to get the mass spectra immediately after introducing the sample.

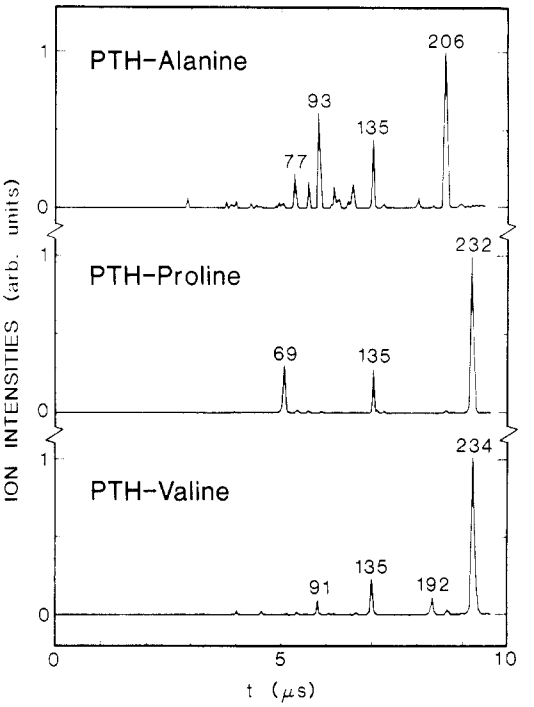

Figure 2. Laser desorption/multiphoton ionization TOF mass spectra of three different PTH-amino acids. In all cases the amounts of PTH-amino acids desorbed by the CO_2 laser (fluence of $\sim$200 mJ/cm^2) is nearly the same ($\sim$5 pg, equivalent to $\sim$1 nmol). The low Nd:YAG laser fluence ($\sim$1 mJ/cm^2) led to dominant parent ion peaks.

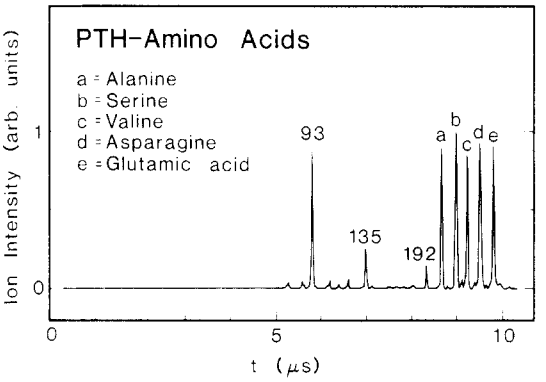

Figure 3. Laser desorption/multiphoton ionization TOF mass spectra of an equimolar mixture of five PTH-amino acids using the same CO_2/Nd:YAG laser fluences as shown in Figure 2.

RESULTS AND DISCUSSION

Typical laser desorption/multiphoton ionization mass spectra of three different PTH-amino acids are shown in Figure 2. The main features are as follows: (i) a high yield of the parent ion peak; (ii) little degree of fragmentation and chemically simple fragmentation paths, i.e., elimination of stable neutral molecules, with the remaining fragment ions still acting as a "fingerprint"; (iii) considerable reduction of background, in contrast to EI, CI, and SIMS, resulting in nearly flat base lines. The spectra shown in Figure 2 are typical for all PTH-amino acids obtained with sample concentration in the subnanomole range. Table II presents the results for 20 PTH-amino acids. For each PTH-amino acid the dominant mass peak (base peak), the abundance of the parent ion peak, and major fragment ions with relative abundance to base peak are reported. It can be seen from Table II that the major fragment pathways yield mass peaks of 192, 135, 93, 91, and 77. Figure 3 shows a typical mass spectra of an equimolar mixture of five PTH-amino acids. The advantage of lower ionizing laser fluence is clearly visible, since the five different PTH-amino acids tested could be

Table II. Main Fragments in the Mass Spectra of PTH-Amino Acids

PTH-amino acids	mol wt	rel abund of M^+, %	base peak, m/e	major fragment peaks (rel abund to base peak in %)
glycine	192	100	192	
alanine	206	100	206	93 (60), 135 (42), 77 (22), 87 (17)
serine	222	100	222	135 (27), 192 (16), 92 (13), 77 (12)
proline	232	100	232	69 (30), 135 (26)
valine	234	100	234	135 (18), 192 (12)
threonine	236	100	236	192 (56), 91 (25), 43 (17), 135 (16)
leucine	248	100	248	135 (40), 219 (13), 192 (12), 43 (10)
isoleucine	248	100	248	192 (40), 135 (33), 57 (17)
asparagine	249	100	249	91 (18), 135 (10)
aspartic acid	250	100	250	135 (21), 91 (17), 85 (17), 119 (11)
glutamine	263	79	93	93 (100, 205 (22), 59 (22), 192 (13)
glutamic acid	264	100	264	135 (15)
methionine	266	100	266	192 (23), 205 (21), 135 (10)
histidine	272	100	272	81 (49), 153 (24), 95 (18), 192 (10)
phenylalanine	282	81	91	91 (100), 131 (98)
cysteic acid	286	27	91	91 (100), 204 (25), 135 (17), 69 (14)
arginine	291	78	93	93 (100), 71 (86), 29 (11)
tyrosine	298	43	107	107 (100), 192 (74)
tryptophan	321	36	130	130 (100), 64 (43), 114 (29), 87 (21)
lysine	398	4	93	93 (100), 305 (72), 69 (50), 26 (30)

completely resolved with our low-resolution TOF mass spectrometer. Moreover, the parent ion signals of all five PTH-amino acids are of comparable size.

Even for PTH-amino acids with the same molecular weight, for example, PTH-leucine and PTH-isoleucine, the fragmentation pattern allows us to distinguish isomers (see Table II). This is in sharp contrast with electron impact ionization (*38*) and chemical ionization (*39*). Moreover, the fragmentation pattern is unique to the PTH-amino acid at low fluences. This has the advantage of allowing identification of PTH-amino acids whose parent ion is nearly absent (see, for example, PTH-lysine and PTH-cysteic acid in Table II).

Velocity Distributions. Varying the time delay between the desorbing CO_2 laser and the ionizing Nd:YAG laser allows us to measure arrival time distributions of the desorbed species. The timing sequence for this kind of measurement needs some description. Briefly the "lamp out" from the Nd:YAG laser served as the master clock for the timing sequence. After a variable delay (0–300 μs) the CO_2 laser was triggered. A NaCl beam splitter and a fast photodiode served to measure the time arrival of the 10-μs pulse from this laser which typically arrived 9 ± 1 μs (function of the input voltage) after the delay generator trigger pulse. The CO_2 laser beam size at the sample was ~0.01 cm^2 and pulse energies of ~50 mJ were used. Pulses from the Nd:YAG laser (typically 1 mJ, 10 ns) arrived after a variable delay and were focused (0.1-cm-diameter beam waist) through the ionization region of the TOF mass spectrometer. The Nd:YAG laser beam (266 nm) propagated 1.2 cm from and parallel to the electrode with the rotating glass cup. An oscilloscope was used to observe simultaneously the arrival of the CO_2 desorption laser pulse, the Nd:YAG ionization laser pulse, and the ion signal.

A typical example (see Figure 4) shows the dependence of the (m/e 192, parent ion) signal on the time delay between the desorption and ionization pulses. The data points—two different runs from different PTH-glycine samples of the same sample film thickness—represent a 100-shot average at each delay for the first run, whereas in the second run they represent single shot at a given delay time. The film thickness of the sample is about 10 monolayers. Similar curves have been measured for other PTH-amino acids with different sample film thicknesses ranging from hundreds of monolayers to submonolayer coverage; they allow interpretation of the mean arrival time as well as the velocity distributions, i.e., kinetic energy distributions of neutral molecules. This is turn gives first insight into the desorption process. Furthermore,

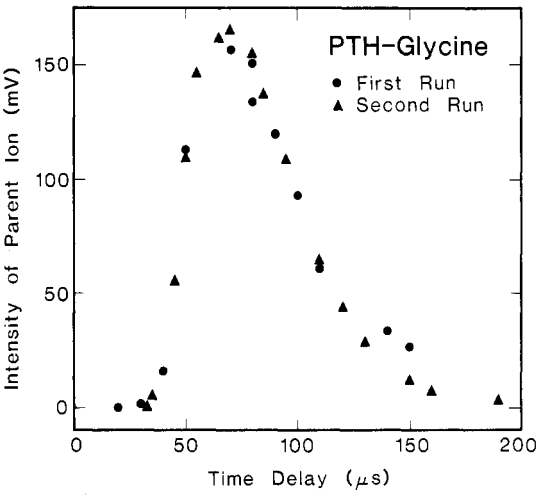

Figure 4. Velocity distribution of PTH-glycine. The ion signal as a function of delay time between CO_2 laser pulse and Nd:YAG laser (266 nm) pulse is given.

our method of detection (MPI) like other laser methods (LIF) is carried out in general by a *density* detector, whereas desorption rates like reaction rates are always related to *flux*. Knowledge of the velocity distribution, i.e., the mean velocity for a given delay time, allows us to determine the *flux* of molecules through our ionization volume.

Following the treatment of Nogar, Estler, and Miller (*30*), we obtain the velocity distribution directly from Figure 4. In the case of PTH-glycine the center-of-mass velocity is 165 ± 5 ms^{-1} and the "thermal" velocity is 177 ± 7 ms^{-1}, which are the same within our experimental uncertainty. Different PTH-amino acids were found to have most probable velocities between 140 and 170 ms^{-1} nearly independent of both the desorption CO_2 laser fluences (50–200 mJ/cm^2) and the thickness of the sample film. The "thermal" velocity distribution was characterized by a width of 180 ± 30 ms^{-1}, corresponding to a "temperature" slightly above room temperature, i.e., 350 K ≤ T ≤ 450 K. Although near-thermal distributions seem to be the norm at least for physisorbed molecules (*40*), nonthermal distributions have also been previously observed (*30*, *41*, *42*).

PTH-serine and PTH-threonine are known to dehydrate upon heating above 400 K (*43*). However, we never observed ions with m/e of 204 and 218, in contrast to electron bombardment (*38*) and chemical ionization (*44*) mass spectrometry.

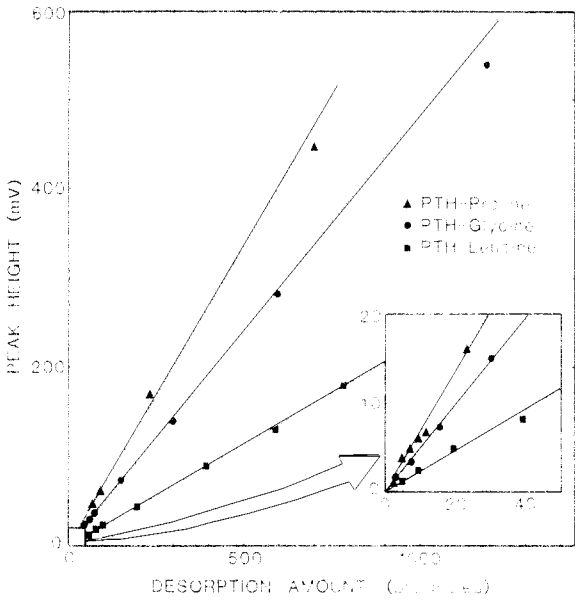

Figure 5. Linearity of response for three selected PTH-amino acids.

This result indicates that desorbed PTH-amino acids escape the substrate rapidly at low temperatures, giving us a clue about the presently unknown nature of the laser desorption mechanism.

Quantitative Analysis. The linear dependence on sample concentration was investigated by using three PTH-amino acids with a fixed CO_2 laser power of 500 kW/cm^2, a fixed Nd:YAG laser power of 1 MW/cm^2, and a fixed time delay between the CO_2 laser pulse and the Nd:YAG laser pulse ($\sim$70 μs). The results are shown in Figure 5 where the maximum output signal for the parent ion, corresponding to the peak height given in millivolts, is plotted against the desorption rate per pulse. The PTH-amino acid concentration ranges over several orders of magnitude between picomole and nanomole. From Figure 5 it should be noted that the linearity of the graphs covers more than 3 orders of magnitude of concentration of PTH-amino acids. The upper limit is due to (a) the nonlinear response of the multiplier and (b) the incomplete desorption of the sample, while the lower limit of about 10^{-12} mol corresponds to a $S/N \simeq 1$ in our analog ion current measurement. We have demonstrated that the desorption is *complete* within the concentration range given in Figure 5, by observing the reduction of mass spectra signal by orders of magnitude in the second rotation on the same circle of a glass cup. With an estimated ionization volume of about 2×10^{-4} L, based on the geometry of the Nd:YAG laser and the TOF mass spectrometer electrodes, about 1 pmol can be detected easily with a satisfactory S/N ratio.

This study is the first quantitative analysis of molecules adsorbed on surfaces by LD/REMPI. In previous work multiphoton ionization has been demonstrated to be quantitative for elemental analysis of surfaces (*29*). Moreover, the present work shows that there is the possibility of lowering the detection limit orders of magnitude below the present level by improvements in the electronics and ion optics.

ACKNOWLEDGMENT

We are grateful to Rachel Schatzberger for assistance.

LITERATURE CITED

(1) *Lasers in Chemical Analysis*; Hieftje, G. M., Travis, J. C., Lytle, F. E., Eds.; The Humana Press: Clifton, NJ, 1981.
(2) *Ultrasensitive Laser Spectroscopy*; Kliger, D. S., Ed.; Academic: New York, 1983.
(3) Keller, R. A., Ed. *Proc. SPIE-Int. Soc. Opt. Eng.* **1983**, *426*.
(4) Zare, R. N. *Science* **1984**, *266*, 298.
(5) Burlingame, A. L.; Baillie, T. A., Derrick, P. J. *Anal. Chem.* **1986**, *58*, 165R.
(6) Rizzo, T. R.; Park, Y. D.; Peteanu, L. A.; Levy, D. H. *J. Chem. Phys.* **1986**, *84*, 2534.
(7) Beckey, H. D. *Principles of Field Ionization and Field Desorption Mass Spectrometry*; Pergamon: New York, 1977.
(8) *Ion Formation from Organic Solids*; Benninghoven, A., Ed.; Springer-Verlag: Berlin, 1983; Part 2.
(9) Posthumus, M. A.; Kistemaker, P. G.; Meuzelaar, H. L. C.; Ten Noever de Brauw, M. C. *Anal. Chem.* **1978**, *50*, 985.
(10) Stoll, R.; Röllgen, F. W. *Org. Mass Spectrom.* **1979**, *14*, 642.
(11) Antonov, V. S.; Letokhov, V. S.; Shibanov, A. N. *Appl. Phys.* **1981**, *25*, 71.
(12) Antonov, V. S.; Letokhov, V. S.; Matveyets, YU. A.; Shivanov, A. N. *Laser Chem.* **1983**, *1*, 37.
(13) Tabet, J.-C.; Cotter, R. J. *Anal. Chem.* **1984**, *56*, 1662.
(14) Egorov, S. E.; Letokhov, V. S.; Shibanov, A. N. *Chem. Phys.* **1984**, *85*, 349.
(15) *Catalyst Characterizaion Science*; Deviney, M. L.; Gland, J. L., Eds.; American Chemical Society: Washington, DC, 1985; pp 238–251.
(16) Karas, M.; Bahr, U. *TrAC, Trends Anal. Chem. (Pers. Ed.)* **1986**, *5*, 90.
(17) Sherman, M. G.; Kingsley, J. R.; Hemminger, J. C.; McIver, R. T., Jr. *Anal. Chim. Acta* **1985**, *178*, 79.
(18) Benninghoven, A.; Sichtermann, W. K. *Anal. Chem.* **1978**, *50*, 1180.
(19) *Secondary Ion Mass Spectrometry SIMS V*; Benninghoven, A., Colton, R. J., Simons, D. S., Werner, H. W., Eds.; Springer Series in Chemical Physics 44; Springer-Verlag: Berlin, 1986.
(20) *Ion Formation from Organic Solids*; Benninghoven, A., Ed.; Springer-Verlag: Berlin, 1983; Part 3.
(21) Blakley, C. R.; Vestal, M. L. *Anal. Chem.* **1983**, *55*, 750.
(22) Vestal, M. L.; Fergusson, G. J. *Anal. Chem.* **1985**, *57*, 2373.
(23) Whitehouse, C. M.; Dreyer, R. N.; Yamashita, M.; Fenn, J. B. *Anal. Chem.* **1985**, *57*, 675.
(24) Conzemius, R. J.; Capellen, J. M. *Int. J. Mass. Spectrom. Ion Phys.* **1980**, *34*, 197.
(25) Hercules, D. M.; Day, R. J.; Balasanmugam, K.; Dang, T. A.; Li, C. P. *Anal. Chem.* **1982**, *54*, 280A.
(26) Hercules, D. M. *Pure Appl. Chem.* **1983**, *55*, 1869.
(27) Antonov, V. S.; Egorov, S. E.; Letokhov, V. S.; Shibanov, A. N. *JETP Lett. (Engl. Transl.)* **1983**, *38*, 217.
(28) Becker, C. H.; Gillen, K. T. *Anal. Chem.* **1984**, *56*, 1671.
(29) Becker, C. H.; Gillen, K. T. *J. Opt. Soc. Am. B: Opt. Phys.* **1985**, *2*, 1438.
(30) Nogar, N. S.; Estler, R. C.; Miller, C. M. *Anal. Chem.* **1985**, *57*, 2441.
(31) Tembreull, R.; Lubman, D. M. *Anal. Chem.* **1986**, *58*, 1299.
(32) Edman, P.; Begg, G. *Eur. J. Biochem.* **1967**, *1*, 80.
(33) Niall, H. D. *Methods in Enzymology*; Academic: New York, 1973; Vol. 73, pp 942–1010.
(34) *Practical Protein Chemistry-A Handbook*; Darbre, A., Ed.; Wiley: Chichester, England, 1986; pp 412–425.
(35) Zimmerman, C. L.; Appella, E.; Pisano, J. J. *Anal. Biochem.* **1977**, *77*, 569.
(36) *Biochemical Applications of Mass Spectrometry*; Waller, G. R.; Dermer, O. C., Eds.; Wiley: New York, 1980; pp 470–474.
(37) Benninghoven, A.; Anders, V. *Org. Mass Spectrom.* **1984**, *19*, 345.
(38) Hagenmaier, H.; Ebbighausen, W.; Nicholson, G.; Vötsch, W. *Z. Naturforsch. B: Anorg. Chem., Org. Chem., Biochem., Biophys., Biol.* **1970**, *25B*, 681.
(39) Fales, H. M.; Nagai, Y.; Milne, G. W. A.; Brewer, H. B., Jr.; Bronzert, T. J.; Pisano, J. J. *Anal. Biochem.* **1971**, *43*, 288.
(40) Burgess, D., Jr.; Viswanathan, R.; Hussla, I.; Stair, P. C.; Weitz, E. *J. Chem. Phys.* **1983**, *79*, 5200.
(41) Comsa, G.; David, R.; Schumacher, B.-J. *Surf. Sci.* **1980**, *95*, L210.
(42) Husinsky, W.; Bruckmüller, R.; Blum, P.; Viehböck, F.; Hammer, D.; Benes, E. *J. Appl. Phys.* **1977**, *48*, 4734.
(43) *Mass Spectrometry, Part A*; Merritt, C., Jr.; McEwen, C. N., Eds.; Marcel Dekker: New York, 1979; pp 28–37.
(44) Fairwell, T.; Brewer, H. B., Jr. *Anal. Biochem.* **1980**, *107*, 140.

RECEIVED for review October 2, 1986. Accepted November 25, 1986. F.E. thanks the Deutsche Forschungsgemeinschaft and Ministerium für Wissenschaft und Forschung des Landes Nordrhein-Westfalen, Federal Republic of Germany, and W.H. thanks the Deutsche Forschungsgemeinschaft for a postdoctoral fellowship.